MID-AMERICA
TRANSPORTATION CENTER

Report # MATC-MU: 181

Final Report
WBS: 25-1121-0003-181

Nondestructive Evaluation Tools to Improve the Inspection, Fabrication and Repair of Bridges

Glenn Washer, Ph.D., P.E.
Associate Professor
Civil and Environmental Engineering
University of Missouri

Steven Brooks, B.S.
Daniel Looten, M.S.

2014

A Coopertative Research Project sponsored by
U.S. Department of Tranportation-Research, Innovation and Technology Innovation Administration

Nondestructive Evaluation Tools to Improve the Inspection, Fabrication and Repair of Bridges

Glenn Washer, Ph. D., P.E.
Associate Professor
Dept. of Civil & Environmental Engineering
University of Missouri

Daniel W. Looten, M.S.
Graduate Research Assistant
Dept. of Civil & Environmental Engineering
University of Missouri

Steven Brooks, B.S.
Graduate Research Assistant
Civil and Environmental Engineering
University of Missouri

A Report on Research ponsored by

Mid-America Transportation Center

University of Nebraska–Lincoln

May 2014

Technical Report Documentation Page

1. Report No. 25-1121-0003-181	2. Government Accession No.	3. Recipient's Catalog No.
4. Title and Subtitle Nondestructive Evaluation Tools to Improve the Inspection, Fabrication and Repair of Bridges		5. Report Date May 2014
		6. Performing Organization Code
7. Author(s) Washer, G., Brooks, S., and Looten, D.		8. Performing Organization Report No. 25-1121-0003-181
9. Performing Organization Name and Address Mid-America Transportation Center 2200 Vine St. PO Box 830851 Lincoln, NE 68583-0851		10. Work Unit No. (TRAIS)
		11. Contract or Grant No.
12. Sponsoring Agency Name and Address Research and Innovative Technology Administration 1200 New Jersey Ave., SE Washington, D.C. 20590		13. Type of Report and Period Covered Final Report. June 2012 to May 2014
		14. Sponsoring Agency Code MATC TRB RiP No. 33541
15. Supplementary Notes		

16. Abstract

The goal of this research project in Nondestructive Evaluation (NDE) is to improve the safety and reliability of bridges through the exploration of three innovative technologies: (1) ultrasonic measurement of in-situ stress levels in gusset plates, (2) evaluation of ultrasonic testing (UT) and phased array testing, and (3) development of vehicle-mounted infrared thermography for bridge condition assessment. The first task investigated a methodology for nondestructive assessment of total stress levels in gusset plates to support safety analysis. This methodology utilizes the acoustoelastic effect to evaluate total stress levels by assessing the acoustic birefringence in the plate. The report describes exploratory testing to evaluate the utility of the approach as a potential tool for the field evaluation of gusset plate adequacy. The second task sought to identify the limitations associated with UT technologies and compare the results to the more recently developed phased array ultrasonic technologies. Various tests were developed to illustrate the limitations of both technologies. Currently, tests are being performed using UT and will be performed using phased array at a later date. In the third task, a flexible, portable platform for infrared thermography that enables the technology to be vehicle-mounted for scanning bridge decks, bridge soffits and tunnels at normal or close to normal traffic speeds was developed although it has not yet been field tested.

17. Key Words Bridge, ultrasonic testing, phased array testing, NDE, acoustoelastic effect, acoustic birefringence, pure-mode polarization directions	18. Distribution Statement		
19. Security Classif. (of this report) Unclassified	20. Security Classif. (of this page) Unclassified	21. No. of Pages 39	22. Price

Table of Contents

List of Figures

Disclaimer

The contents of this report reflect the views of the authors, who are responsible for the facts and the accuracy of the information presented herein. This document is disseminated under the sponsorship of the U.S. Department of Transportation's University Transportation Centers Program, in the interest of information exchange. The U.S. Government assumes no liability for the contents or use thereof.

Abstract

The goal of this research project in Nondestructive Evaluation (NDE) is to improve the safety and reliability of bridges through the exploration of three innovative technologies: (1) ultrasonic measurement of in-situ stress levels in gusset plates, (2) evaluation of ultrasonic testing (UT) and phased array testing, and (3) development of vehicle-mounted infrared thermography for bridge condition assessment. The first task investigated a methodology for nondestructive assessment of total stress levels in gusset plates to support safety analysis. This methodology utilizes the acoustoelastic effect to evaluate total stress levels by assessing the acoustic birefringence in the plate. The report describes exploratory testing to evaluate the utility of the approach as a potential tool for the field evaluation of gusset plate adequacy. The second task sought to identify the limitations associated with UT technologies and compare the results to the more recently developed phased array ultrasonic technologies. Various tests were developed to illustrate the limitations of both technologies. Tests are currently being performed using UT, and will be performed using phased array at a later date. In the third task, a flexible, portable platform for infrared thermography that enables the technology to be vehicle-mounted for scanning bridge decks, bridge soffits, and tunnels at normal or close to normal traffic speeds was developed, although it has not yet been field tested.

Chapter 1 Introduction

The goal of this research project in Nondestructive Evaluation (NDE) is to improve the safety and reliability of bridges. Three innovative technologies are the focus of the research described in this report:

1) Ultrasonic Measurement of In-Situ Stress Levels in Gusset Plates

   Measure the actual in-situ stress levels in the gusset plates to ensure structural safety (chapter 2)

2) Development of Phase Array Ultrasonic Testing (UT) for Steel Fabrication

   Improve the quality control process for steel fabrication to improve the reliability, safety, and quality of welded constructions (chapter 3)

3) Vehicle-Mounted Infrared Thermography for Bridge Condition Assessment

   Develop a flexible, portable platform for infrared thermography that enables the technology to be vehicle-mounted for scanning bridge decks, bridge soffits, and tunnels at close to normal traffic speeds (chapter 4)

This experimental research explored that application of these technologies for practical applications for bridge condition assessment. The results of this research will enhance the safety of the transportation infrastructure by providing better tools for the safety condition assessment of bridges during fabrication, inspection, and repair. The research will also enhance the state of good repair by developing technologies for detecting deterioration in its embryonic stages, when maintenance and preservation strategies can be implemented to ensure the state of good repair. The benefit is better, safer, and longer-lasting steel and concrete bridges and related structures.

Chapter 2 Ultrasonic Biaxial Stress Measurement for Evaluating the Adequacy of Gusset Plates

2.1 Introduction

2.1.1 Goals and Objectives

The overall goal of this research task is to improve the safety of highway bridges by identifying over-stressed steel gusset plates. The objectives of this research task are to:

- assess the effect of texture direction on ultrasonic shear wave velocities,
- evaluate the accuracy and precision of ultrasonic stress measurements for a biaxial stress condition, and
- develop an ultrasonic stress measurement methodology for determining total stress in steel gusset plates in-situ.

2.1.2 Motivation

The need for improved condition assessment technology became evident when the I-35W bridge in Minneapolis, Minnesota, collapsed. The accident occurred during the afternoon rush hour on August 1, 2007, resulting in the deaths of 13 people [1]. Figure 2.1 is a photograph of the collapse site.

Figure 2.1 Collapsed I-35W bridge section [1]

An investigation of the collapse by the National Transportation Safety Board (NTSB) indicated the cause of the collapse was the failure of an overloaded steel gusset plate connecting key members of the structure. The gusset plate, shown in figure 2.2, was not of adequate thickness to carry the applied loads given its configuration, though it had performed adequately since the construction of the bridge in 1967.

Factors that may have contributed to the failure of the gusset plate include additional dead load applied to the structure over time due to rehabilitation activities, as well as construction loading due to ongoing operations [1].

Figure 2.2 Photograph from 2003 of the failed gusset plate [1]

2.1.3 Discussion

Since the time of the collapse, State Departments of Transportation and other bridge owners have struggled to determine if existing gusset plates are adequate to carry applied loading and ensure bridge safety. To assess the adequacy of a given plate to carry required loads, the

actual forces acting on the plate are needed to compare to the calculated capacity of the plate. The complex nature of force distributions in large truss bridges results in significant uncertainty in the level of stress carried by individual bridge members and, consequently, the required stresses in the gusset plates connecting the members. Figure 2.3 demonstrates the complexity of the stress field experienced by a gusset plate. Currently, no methodologies exist that can measure total stress (i.e., the combination of stresses resulting from dead load, live load, residual effects, etc.) throughout the entire thickness of the material. For example, strain gages can only measure surface strains and cannot account for the inherent strain present before the installation of the gage.

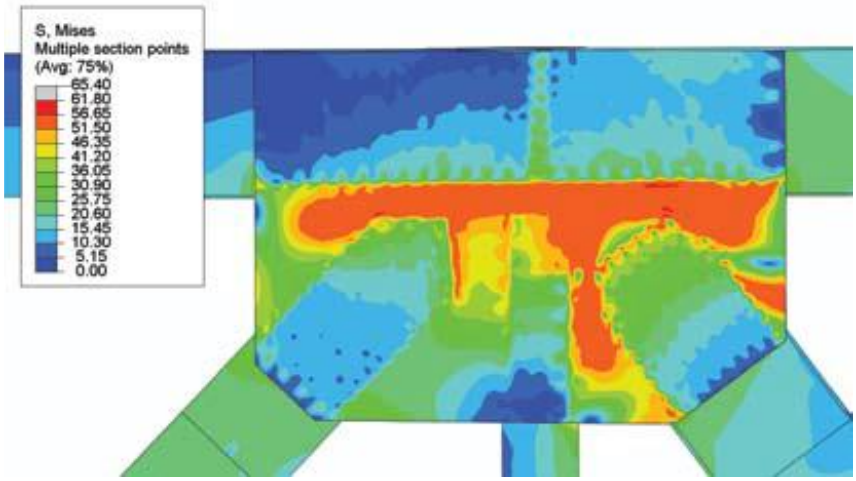

Figure 2.3 Finite element model of the failed gusset plate demonstrating the complex stress field experienced by a gusset plate [1]

In this research, an ultrasonic stress measurement methodology is being developed to evaluate the actual stress level in a gusset plate. The approach uses ultrasonic birefringence as a means of assessing the stresses carried in the plate. The ultrasonic birefringence approach is a nondestructive technique based on the acoustoelastic effect (i.e., the variations in ultrasonic wave

velocity as a result of strain). Measurements from the ultrasonic birefringence approach can determine the total combined stresses resulting from dead load, live load, and residual stresses. The developed methodology could have a significant impact on the current standards for evaluating bridge capacities and enable more reliable assessments to ensure bridge safety nationwide.

2.2 Background and Theory

2.2.1 Measurement Using Ultrasonic Waves

Ultrasonic testing (UT) is a NDE method that uses mechanical waves at ultrasonic frequencies to detect or measure certain characteristics of structural components. UT is often used as a bulk measurement technique in which mechanical waves propagate through the thickness of the material, making characterization of the entire material possible. For the UT measurement of stress in a gusset plate, shear horizontal (SH) waves are used.

Ultrasonic waves propagate at a certain velocity depending on the elastic properties of a material (i.e., modulus of elasticity, elastic constants, density, and Poisson's ratio). However, the elastic constants for a given material are a function of the strain in the material; therefore, when a material is strained (or stressed), the velocity of an ultrasonic wave is altered.

2.2.2 Acoustoelastic Effect

The *acoustoelastic effect* expresses variations in the elastic properties of the material resulting from applied strains through the effect on the velocity of an acoustic wave. The change in velocity of an acoustic wave is very small (less than 1% of the velocity in the unstressed material), but the effect is large enough to be accurately measured. When a shear wave propagates through an isotropic, homogeneous medium, it propagates at a single velocity regardless of the polarization direction of the wave. However, when a material is anisotropic, or

when stress is introduced, the velocity of the shear waves will become dependent on the polarization orientation of the wave.

2.2.3 Acoustic Birefringence

Another way to utilize this effect is to analyze differences in the velocity of orthogonally polarized shear waves – an effect known as *acoustic birefringence*. Acoustic birefringence measurements can be obtained by the measurement of velocities of the two separate shear waves, one propagating in the "fast" direction and the other propagating in the "slow" direction. These orientations are known as the *pure-mode polarization directions*. The normalized acoustic birefringence, B, can be determined from the equation

$$B = \frac{V_f - V_s}{V_{avg}} \tag{2.1}$$

where V_f is the velocity of the fast wave, V_s is the velocity of the slow wave, and V_{avg} is the average velocity [2].

It is important to note that such a measurement is independent of thickness because each wave propagates over the same distance, with the difference between those measurements being transit time. As such, the material thickness, or travel path of the waves, is eliminated from the determination of the birefringence.

2.2.3.1 Natural Birefringence

Anisotropy in steel can result from a texture effect caused by rolling processes during fabrication, such that there is a "natural" birefringence effect in the plate when stresses are nominally zero. In the absence of stress, the pure-mode polarization directions will be coincident with the rolling and transverse directions of the plate due to the rolling process. This process

gives a texture to the material by elongating all of the grains in a preferred orientation. The rolling, or texture, direction is easily determined in a texture test where the wave polarization direction is rotated at incremental angles, totaling 360°. Wave velocity measurements are recorded at each angle. The results of three such tests are shown in figure 2.4, where the rolling direction is indicated by maximum wave velocities at polarization angles of 90° and 270°. Velocity measurements were recorded at 20° increments.

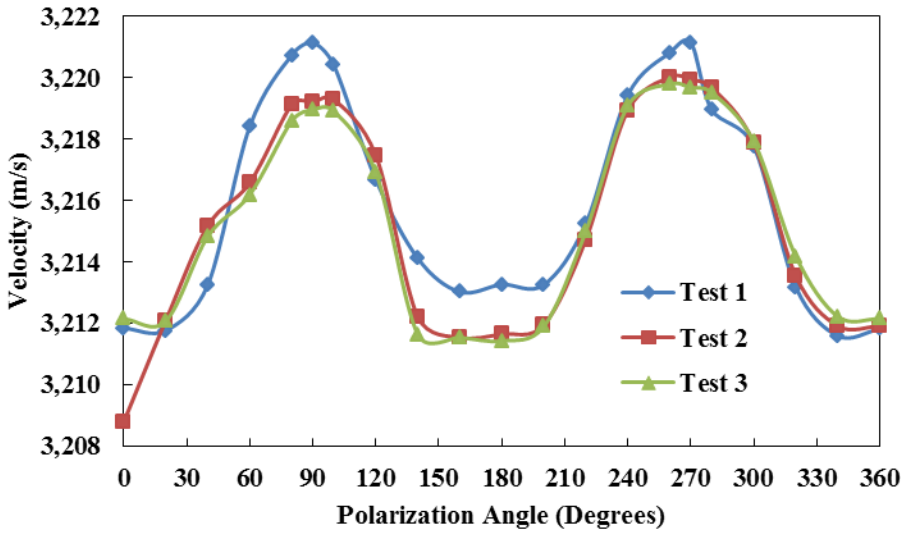

Figure 2.4 Results of a texture test on a hot-rolled steel specimen [3]

2.2.3.2 Pure-Mode Polarization Directions

The presence of shear stress, σ_{xy}, in the direction of rolling will cause a rotation of the pure-mode polarization directions through the angle ϕ [2]. This phenomenon is illustrated in figure 2.5, where the X_0 and Y_0 axes represent the rolling and transverse directions, and the X and Y axes represent the pure-mode polarization directions. Figure 2.6 demonstrates the phase shift of the texture test curves due to the presence of shear stress in the rolling direction.

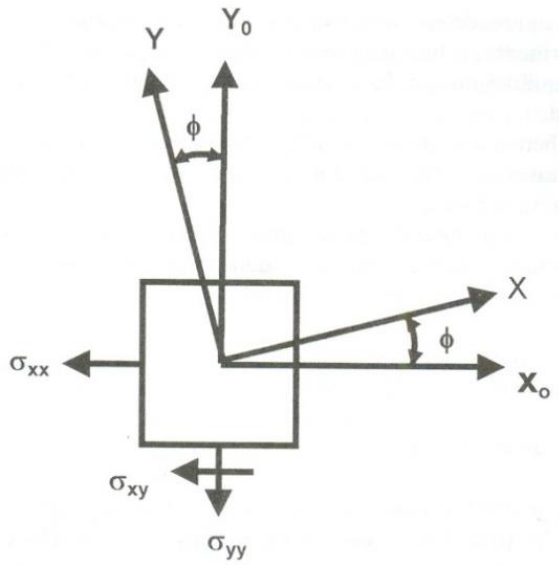

Figure 2.5 Rotation of the pure-mode polarization directions with respect to the rolling and transverse directions due to the presence of shear stress [4]

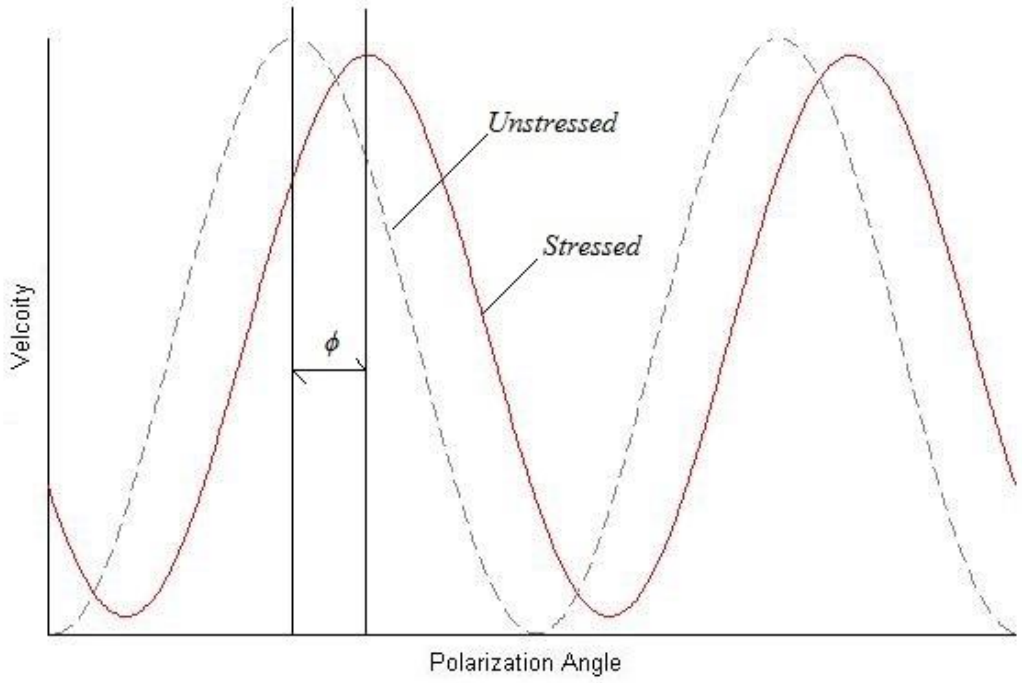

Figure 2.6 Effect of shear stress on the results of a 360° wave velocity test

2.2.4 Stress-Birefringence Relationship

The relationship between birefringence and stress is expressed by the equation

$$B = \left\{\left[B_0 + k\left(\sigma_{yy} - \sigma_{xx}\right)\right]^2 + \left(2k\sigma_{xy}\right)^2\right\}^{1/2} \tag{2.2}$$

where B_0 is the natural birefringence of the material in the unstressed state, k is the stress-acoustic constant (k = 6.34 (10^{-8}) psi^{-1} for A-36 steel), and σ_{xx}, σ_{yy}, and σ_{xy} are the in-plane stresses in reference to a coordinate system aligned with the steel rolling and transverse directions [2].

The phase shift of the pure-mode polarization directions, ϕ, caused by the presence of shear stress, σ_{xy}, is given by

$$\tan 2\phi = \frac{2k\sigma_{xy}}{B_0 + k\left(\sigma_{yy} - \sigma_{xx}\right)} \tag{2.3}$$

Combining equations 2.2 and 2.3 and using trigonometric identities yields

$$\sigma_{xy} = \frac{B \sin 2\phi}{2k} \tag{2.4}$$

$$\sigma_{yy} - \sigma_{xx} = \frac{B \cos 2\phi - B_0}{k} \tag{2.5}$$

which will serve as the model used for experimental testing during this research.

2.3 Experimental Testing

This section will discuss the experimental setup and methods that will be applied to demonstrate the effect of texture on shear wave velocity measurements and to determine the accuracy and precision of measured stresses using equation 2.4 and equation 2.5 as a model.

2.3.1 Experimental Setup

The experimental setup is divided into four parts: steel specimens, applied loading, ultrasonic instrumentation and measurement, and strain measurement. Biaxial loading will be applied to two unique steel plate specimens. The stress state of the steel will be measured using UT and subsequently compared to strain gage stress measurements.

2.3.1.1 Steel Specimens

Two 12”x4”x0.25” A-36 steel specimens were fabricated for testing, as shown in figure 2.7. Each specimen has a unique texture direction specifically designed for the loading configuration in this experiment: one with the texture direction coincident with the major principal stress axis (normal texture direction) and one with the texture direction diagonal to the major principal stress axis (diagonal texture direction). As such, the normally textured plate will not have shear stress in the plane of texture, while the diagonally textured plate will have shear stress in the plane of texture. This allows for the effect of shear stress in the texture plane to be demonstrated as described in section 2.2.3.2 of this report. Holes were drilled at both ends of each specimen for pin and clevis connections. The plates were specifically designed (i.e., the distance between pinholes) to diminish the stress concentration due to the holes and to achieve a uniform stress field at the center of the plate where UT measurements will be taken.

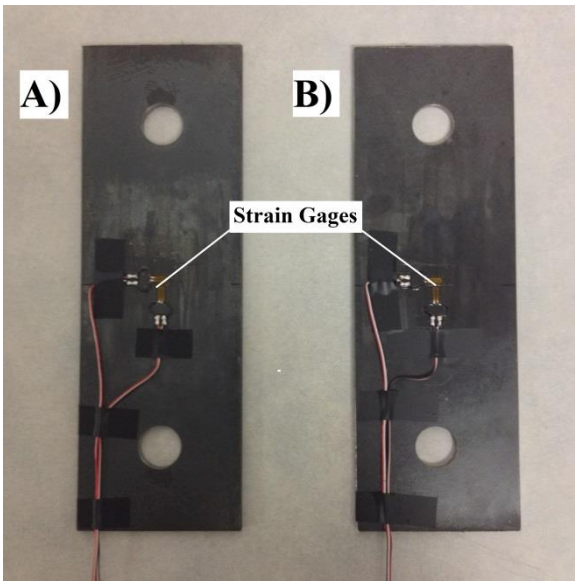

Figure 2.7 Steel plate specimen with a normal texture direction (A) and a diagonal texture direction (B)

2.3.1.2 Applied Loading

The steel specimens are to be tested under a biaxial loading condition to simulate the loading experienced by a bridge gusset plate. A tensile force will be applied in the vertical direction using pin and clevis connections fixed to the loading machine shown in figure 2.8. A load-control program has been designed using LabView software in which the desired static load and ramp time are input to achieve the preferred loading condition.

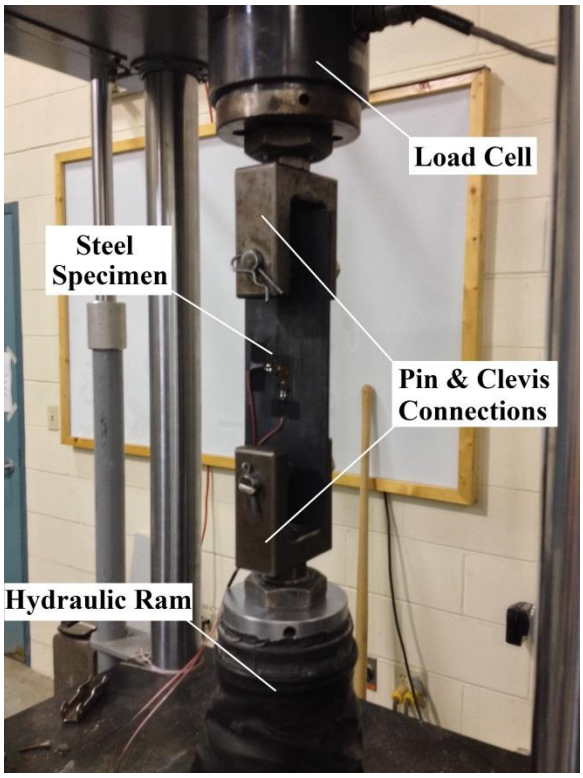

Figure 2.8 Loading machine with pin and clevis fixtures

For lateral loading, a steel load frame has been designed and built to apply compressive force to the plate. The load frame, shown in figure 2.9, consists of two steel bearing plates connected by four stainless steel shafts with threaded ends. Nuts and washers are attached to the ends of each shaft; the amount of compressive force is controlled by torqueing each nut. To prevent bending of the plate, an equal amount of tensile force must be present in each shaft. Strain gages have been installed on each shaft to monitor the strains and ensure the forces applied to each shaft are approximately equal.

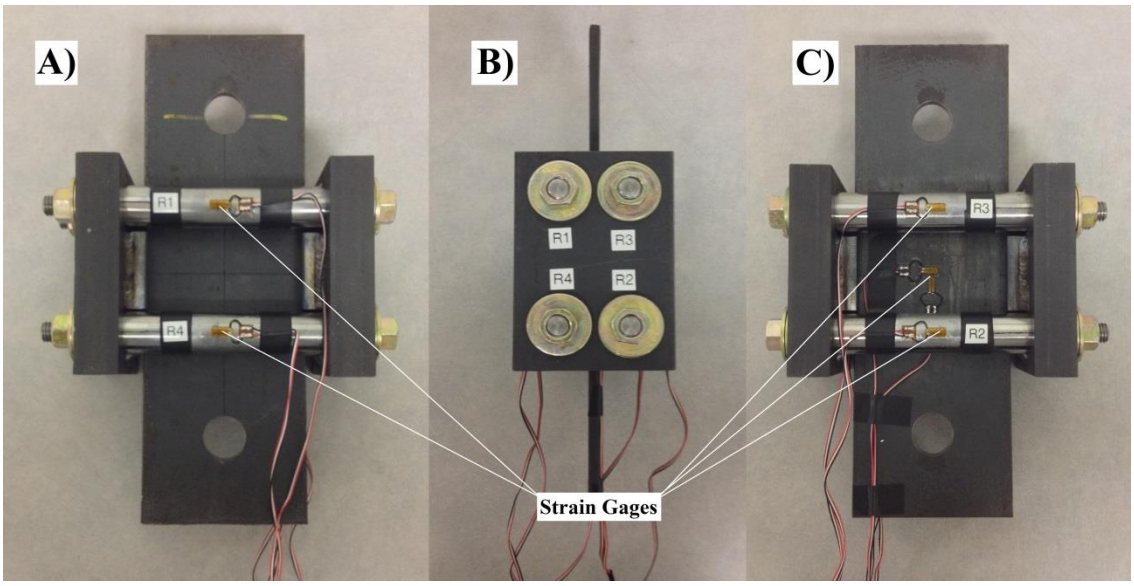

Figure 2.9 Lateral loading frame, as seen from the front (A), side (B), and rear (C), fastened to a steel plate specimen

2.3.1.3 Ultrasonic Instrumentation and Measurement

Figure 2.10 shows three essential pieces of hardware used for UT: a high-speed digital oscilloscope, a high-powered pulser-receiver unit, and an electromagnetic acoustic transducer (EMAT). The pulser-receiver to be used for testing is the Powerbox H made by Innerspec Technologies, which can provide up to 8 kW of power. Pulses generated by the pulser-receiver are sent to the EMAT, which creates shear waves that propagate through the material thickness and reflect off the back surface. Echoes are then sensed by the EMAT, and the response is returned to the pulser-receiver. The waveform is subsequently displayed on the oscilloscope and can be saved to the hard drive. The saved signals can then be exported to specially designed timing software for analysis. For this research, 360° wave velocity tests will be performed under various levels of loading, with measurements being taken at 22.5° increments.

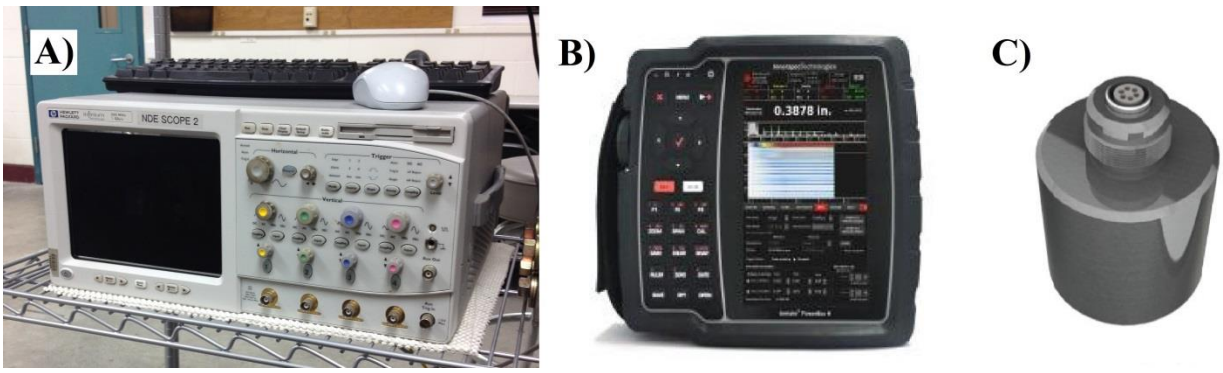

Figure 2.10 Ultrasonic instrumentation consisting of a digital oscilloscope (A), a high-powered pulser-receiver unit (B), and an EMAT sensor (C)

2.3.1.4 Strain Measurement

Resistance-type strain gages will be used in this research to determine the stress state of a specimen under biaxial loading. These measurements will serve as a basis for comparison to the UT stress measurements in order to comment on the accuracy of the stress-birefringence model. The circuit board shown in figure 2.11 has been assembled to allow for multiple strain gage measurements simultaneously. As shown in figure 2.7, two gages are mounted on each specimen, one oriented vertically and one oriented horizontally, to measure strain in the principal directions. Using elastic properties of steel, the strains will be converted into stresses, and stress transformations can then be applied to determine the state of stress for any orientation. The orientation of interest for this experiment will be the pure-mode polarization directions, as determined from UT.

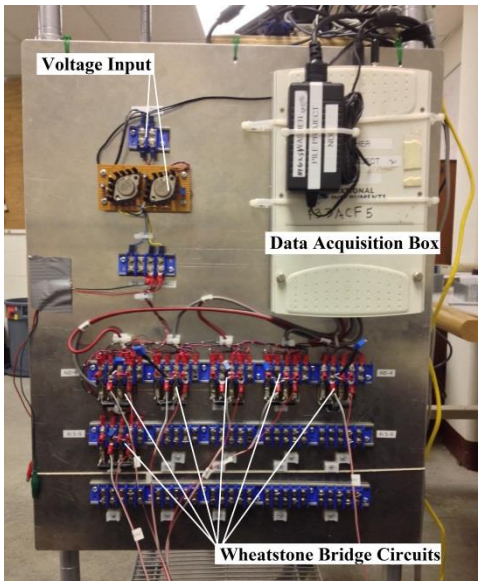

Figure 2.11 Circuit board for the simultaneous operation of multiple strain gages

2.3.2 Data Reduction

After the ultrasonic signals are acquired, they must be processed in order to determine the shear wave velocity. The series of velocity measurements must then be reduced into a simplified and usable form to obtain the desired parameters (i.e., the magnitude and location of the pure-mode polarization velocities).

2.3.2.1 Velocity Measurements

Signals stored within the oscilloscope will be post-processed using specially designed software that enables sub-interval timing of the digital signal. Figure 2.12 is a screenshot of the graphical user interface of the software. The program, like the oscilloscope, displays the voltage on the vertical axis and time on the horizontal axis. A time range for the start and end gate, typically the first and third echoes, are selected from the waveform so that the time-of-flight (or velocity) of the signal can be determined. Once the signal crosses the user-defined voltage threshold, the gates are set and the time-of-flight is measured. The software then calculates the

wave velocity based on the user-defined travel distance. This process will be repeated for each saved waveform.

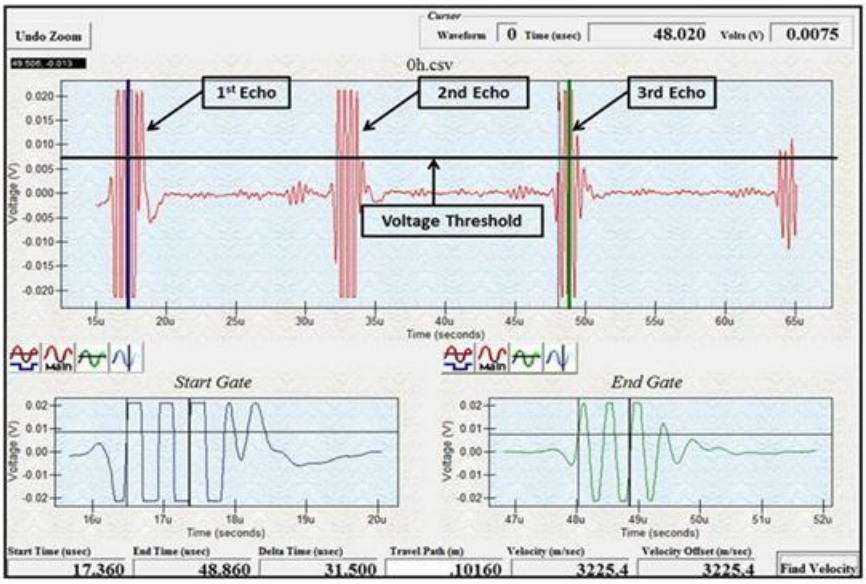

Figure 2.12 Graphical user interface of the specially designed timing software

2.3.2.2 Birefringence and Phase Shift Measurements

Once the velocities are measured, a plot of wave velocity versus polarization angle can be produced for each level of loading. Using a program designed in MATLAB, a sine regression curve with a fixed 180° period is fit to the data. One such plot is shown in figure 2.13. A fixed period is necessary in order to accurately measure the phase shift, ϕ, between curves in a stressed state versus an unstressed state. Using equation 2.1, the birefringence parameter, B, is determined from the normalized difference between the maximum and minimum of the regression curve (i.e., the fast wave velocity, V_f, and the slow wave velocity, V_s). These parameters can then be used to determine the stress state based on equation 2.4 and equation 2.5.

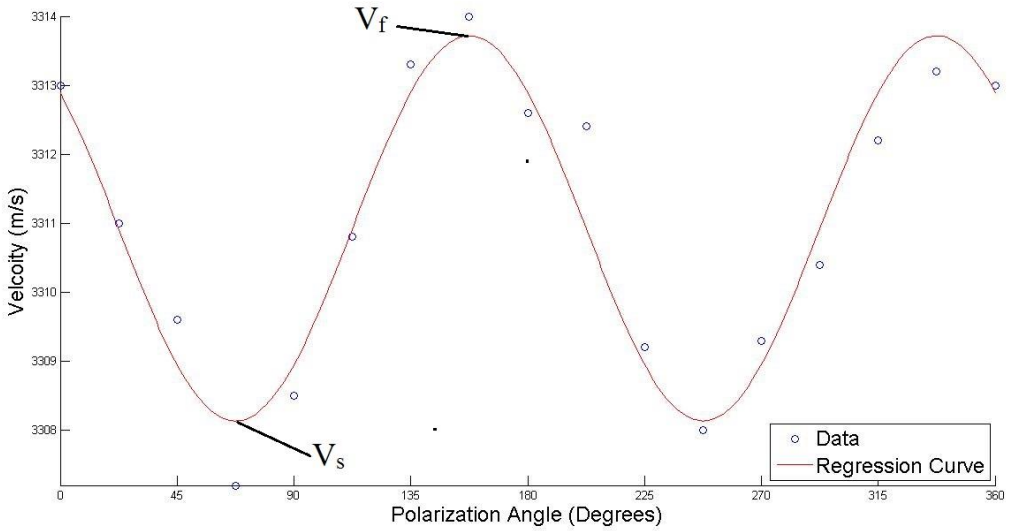

Figure 2.13 Sine regression plot produced by the MATLAB sine regression program

2.3.3 Anticipated Outcomes

The experimental design and setup has been completed. No significant data can be reported at this time. The Powerbox H pulser-receiver unit has been ordered, and testing will commence upon arrival of the unit.

The objectives of the experimental testing include the demonstration of the phase shift of the pure-mode polarization directions due to the presence of shear stress and a comparison of the ultrasonic stress measurements with strain gage measurements. Statistical analysis of the results will be performed to quantify the accuracy and precision of the UT measurements. Upon completion of this research, all major principles of ultrasonic stress measurement will be demonstrated and an understanding of the accuracy of the stress-birefringence model will be established. Future work will include field implementation of the technology.

Chapter 3 Evaluating Ultrasonic Testing and Phased Array Testing

3.1 Goals and Objectives

3.1.1 Introduction

NDE technologies, such as ultrasonic testing (UT), are required quality control tools used in the manufacturing process of welded steel bridge components [5]. These technologies are also used for in-service evaluation of the components to identify defects within the welded region. These defects include fatigue cracks that may have developed from traffic loads and various types of flaws within steel welds, such as lack of fusion, heat affected zone cracks, and slag inclusion. UT relies on trained technicians implementing the procedures and interpreting the results to identify and characterize defects. As a result, variations can occur between inspector conclusions [6-8].

3.1.2 Goals and Objectives

The goal of the test procedures is to improve the safety and reliability of steel structures. The objective of the testing is to improve the results of the American Welding Society (AWS) UT procedure by identifying the limitations of the UT procedure, identify the limitations of phased array UT, and suggest updates to the AWS UT procedure.

3.1.3 Scope

The test requirements for inspecting steel welds in bridges are outlined in the AWS Bridge Welding Code [5]. Due to the variability of the inspectors using the AWS UT procedure, it is necessary to evaluate the reliability of UT.

This research will develop phased array technologies to improve the safety and quality of welded constructions. The research will explore the relationship between the capabilities of the UT and phased array UT technologies and requirements for flaw detection and characterization.

Under this task, test specimens with embedded flaws will be assessed using both traditional ultrasonic technologies, and the recently developed phased array technology. These specimens have been fabricated with embedded flaws typically encountered during the fabrication and welding process. The reliability of the two approaches will be evaluated and compared, and procedures for utilizing the new technology to improve the reliability of steel bridges will be developed.

3.2 Background

3.2.1 UT Procedure

UT is a volumetric NDE that enables subsurface inspection of steel welds. UT consists of sending high-frequency acoustic waves into the volume of the steel weld. Any reflected wave is the product of a discontinuity within the weld. These discontinuities include cracks, porosity, slag inclusions, and rough edges of the steel. The UT D1.5 code is used for UT inspection of bridges. The UT section of the code was developed in the late 1960s and remains mainly unchanged. The code encompasses inspection procedure, equipment calibration, and defect acceptance criteria.

UT consists of launching a high-frequency acoustic wave into the welded region of a steel component, and interpreting received signals (reflections) to assess if there are flaws in the weld, such as porosity, lack of fusion, or cracking. UT is a volumetric NDE technology that enables the detection and characterization of subsurface features, such as flaws along the weld fusion line, subsurface cracks, etc. For bridges, UT is typically conducted in accordance with the AWS code section D1.5 [5]. This code was first developed in 1969, and remains largely unchanged [9]. The specification identifies items such as required training, equipment,

calibration of instruments, and assessment of indications. Figure 3.1 shows an ultrasonic transducer being used to detect a defect in a steel weld.

Figure 3.1 Photograph of an ultrasonic transducer detecting a defect in a steel weld

The AWS D1.5 uses UT to characterize subsurface defects in steel welds by assessing the reflected amplitude and length of defects. The AWS UT procedure uses an identification rating by adjusting the measured defect amplitude in respect to a reference amplitude and an attenuation factor. The reference amplitude is the measured amplitude from a calibration block with a 1/16" diameter hole. The attenuation factor accounts for the amount of wave energy that dissipates as the acoustic wave travels into the steel. The relative amplitude of the indication is measured in dB and can be calculated as follows:

$$dB\ rating = 20log(A_1/A_0) \qquad (3.1)$$

where A_0 is the initial amplitude, and A_1 is the amplitude of the signal being assessed.

Once the identification rating of a defect is determined, the amplitude and length of the defect is compared to the acceptance criteria listed in the AWS code. Defects are classified into categories of A, B, C, or D. Indications identified in Class A are always rejectable, regardless of length, while indications identified in Class B and C are only rejectable if the length of the indication exceeds certain values; Class D indications are acceptable, regardless of length. To determine the length of the indication, the edges are identified where the measured amplitude drops 50% (-6 dB change). The length and indication rating are then compared with the acceptance criteria specified in the AWS code. The amplitude ratings differ by only 5 dB between a Class A indication and a Class D indication for plates at least 1.5 in. thick under tensile stress; for plates less than 1.5 in. thick, the amplitude ratings differ by only 3 dB. [6]

3.2.2 UT Reliability Literature Search

The effectiveness of UT relies on the diligence of the technicians. For example, Gruber and Light tested the reliability of inspectors using the AWS D1.1 Code to assess welded moment frame joints. Twelve mockup specimens containing a total of 17 flaws were inspected by an operator using the AWS D1.1 procedure. Results were assessed to determine the number of known flaws not detected by the inspectors, or "missed indications," as well as indications reported where no flaw exists, or "false alarms." In the testing, there were 17 defects; results showed 4 missed indications and 13 false alarms [7].

Shaw performed an evaluation of reliability on UT in which 15 UT technicians inspected 12 welds with embedded defects. In total, there were 222 tests on known flaws, with 56 missed indications, 166 detections, and 32 false alarms [8].

Another study evaluated 14 known flaws assessed by 3 different inspectors, and rated according to the AWS procedure for acceptable or reject able indications. Eight of the flaws were

rejected by all inspectors (58%), and there was disagreement on the accept/reject decision for five of the flaws (35%) [6]. Additionally, the amplitude rating measured during the testing varied on average 6.5 dB, indicating high variability in a key parameter used to classify a given indication as rejectable or acceptable.

3.2.3 Sherman-Minton Performance Test

A performance test was conducted during the inspection of the Sherman-Minton Bridge as a means of ensuring the inspectors were capable of providing consistent results when identifying and characterizing cracks in steel welds. The operators were instructed to follow procedures generally based on the AWS D1.5 code in their inspections and inspect test specimens containing known defects. The maximum reflected amplitude, the flaw length and the flaw location were recorded and analyzed. The results were then compared using a reliability rating system developed in prior UT research [10].

The results of the performance test revealed inconsistencies in the reported amplitudes and flaw length measurements. Error as a percentage of flaw length was greatest (110%) for the short flaw, and least for the longest flaw (15%). It was concluded from these results that the UT procedure generally overestimated the length of small flaws, and its accuracy increased as the flaw length increased. Results from the UT testing also revealed that "repeat" calls, where an indication is reported more than once, occurred several times during the testing.

3.3 Equipment

3.3.1 Test Setups

Initially, the Instek GDS-2104 100 MHz 4 Ch Visual Persistence Digital Storage Oscilloscope was used to gather waveform data. The oscilloscope was capable of saving waveforms to a .csv file for later analysis, but the data acquisition was slower than what was

required. In order to gather information more quickly, an encoder was required to associate each waveform with a location. This capability was particularly important in the length-amplitude, transducer orientation, defect orientation and defect sizing tests. The USB-UT350 pulser-receiver was ordered to replace the Instek GDS-2104 for this research. In order to incorporate encoder readings, the USB-UT350 pulser-receiver was obtained.

3.3.2 Transducer

The research used a contact shear wave piezoelectric transducer to pulse and receive acoustic shear waves at a frequency of 2.25 MHz. The probes include 0.625" x 0.625" transducers attached to the AWS 70°, 60°, and 45° acrylic wedges.

3.3.3 Encoder

The research used a S1 encoder during the ultrasonic measurements to associate the UT waveforms to locations along the movement path. A contact wheel was secured to the encoder axel to associate a rotation to a distance. The encoder sent a signal to the USB-UT350 each time the encoder axel rotates. The USB-UT350 received both the encoder location and ultrasonic waveform signals simultaneously. These signals were saved to a spreadsheet file for analysis.

3.3.4 USB-UT350

The AWS angle-beam ultrasonic transducer and S1 encoder were connected to the USB-UT350 pulser-receiver. The USB-UT350 was connected to a laptop where the UT waveform was displayed on an oscilloscope, and the encoder data was also displayed. A LabView program was developed to receive the waveforms from the USB-UT350 and translate the waveform data to a spreadsheet format for later analysis.

3.4 Experiment

3.4.1 Test Procedures

Because the AWS relies on the pulse-echo technique for UT, these tests are used to determine what factors impact the reflected amplitude. The tests include: length-amplitude measurement, size-amplitude measurement, transducer wedge angle-amplitude measurement, transducer orientation-amplitude measurement, defect orientation-amplitude measurement, surface roughness-amplitude measurement, attenuation measurements, and defect sizing using AWS procedure. Four steel specimens used for testing included fabricated test plates with implanted flaws. Three plates had transition welds and one plate was a standard butt weld. Other steel specimens used for each test were customized to fit each test's requirement.

3.4.1.1 Length-Amplitude Measurement

The purpose of the length-amplitude test is to identify the accuracy of the current AWS UT flaw length measurement procedure.

In order to characterize the length of a defect in steel welds, the UT associates a 50% drop in max UT amplitude as a threshold at which a defect edge exists. The results from the Sherman-Minton Bridge performance evaluation found that when the defect length is smaller than the size of the transducer, the length determined by the technician is much longer than the actual defect length [10]. When the transducer scans a defect smaller than the transducer, the entire defect will be encompassed in the transducer scan, as seen in figure 3.2. The defect is completely encompassed in the scan, resulting in an extension of length at which maximum amplitude is attained. This research looks to determine the defect lengths at which AWS wedge transducers are overestimated.

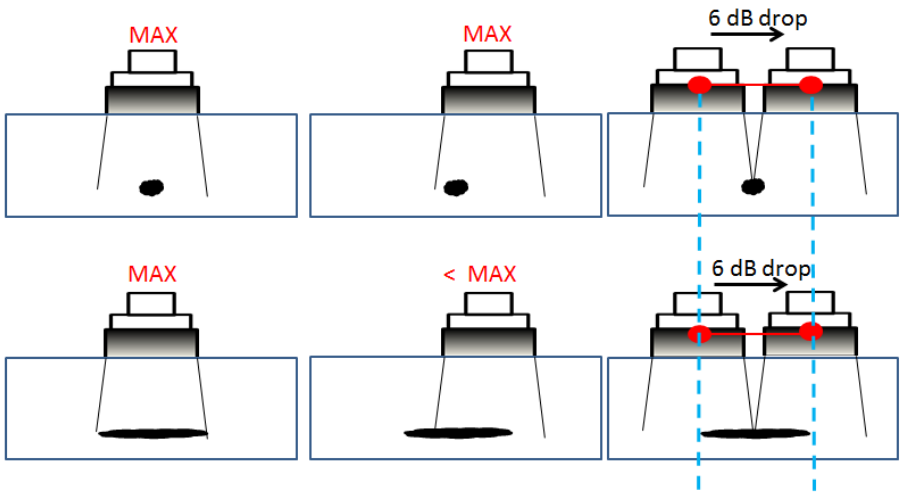

Figure 3.2 Drawing of the acoustic wave when measuring defects smaller than the transducer

The specimen used in the length-amplitude test is made of A36 steel, 1" thick 12"x12" with eight different EDM cuts of varying lengths, as seen in figure 3.3. Four slots were cut through the steel at different lengths. Three grooves were made in the steel to resemble fatigue cracks. One 1/16" diameter hole was made through the plate. The defect lengths were designed so that some defect sizes were smaller and some defect sizes were larger than the transducer.

An encoder will be used to track the waveforms as the transducer moves parallel to the defect. As the defect is being scanned, the transducer creates waveforms that are being associated with the location of the encoder. When the scan is finished, the data points are written to a spreadsheet for evaluation. The encoder allows the waveforms to be mapped back to the transducer position and the defect location. A visual representation of the waveform along with the defect location make is used in the evaluation flaw measurement procedure.

3.4.1.2 Size-Amplitude Measurement

The purpose of the defect size-amplitude test is to relate the size of known defects to the reflected amplitude.

As explained earlier, the UT procedure incorporates a reference amplitude that is used in the evaluation of steel welds. The AWS UT acceptance criteria are based on the reference amplitude measured from the 1/16” hole in the calibration blocks. The measured defect amplitude is compared to the amplitudes listed in the AWS acceptance criteria to determine the severity of the defect. The defect size test looks to quantify the relationship between defect size and the reflected amplitude and compare the results to the current AWS UT code.

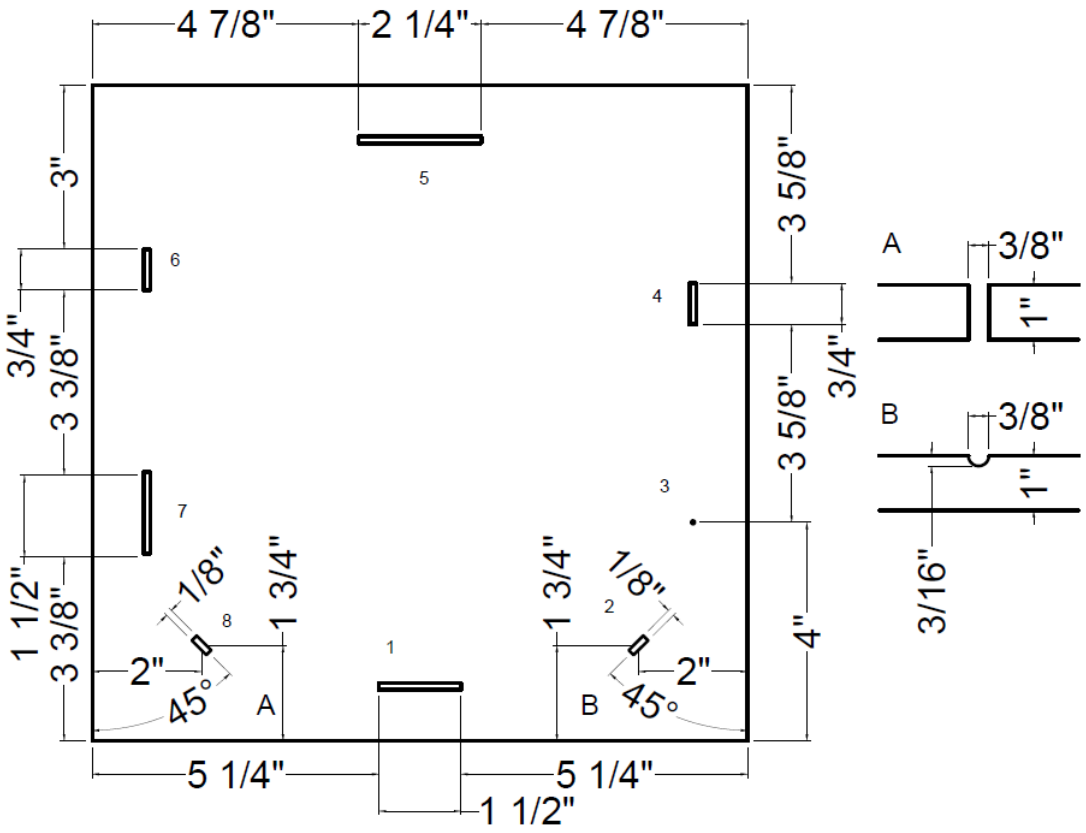
4 7/8"
2 1/4"
4 7/8"
3"
3/4"
3 3/8"
1 1/2"
3 3/8"
3 5/8"
3 5/8"
3/4"
4"
1 3/4"
1 3/4"
1/8"
1/8"
2"
2"
45°
45°
A
B
5 1/4"
5 1/4"
1 1/2"
A
3/8"
1"
B
3/8"
1"
3/16"

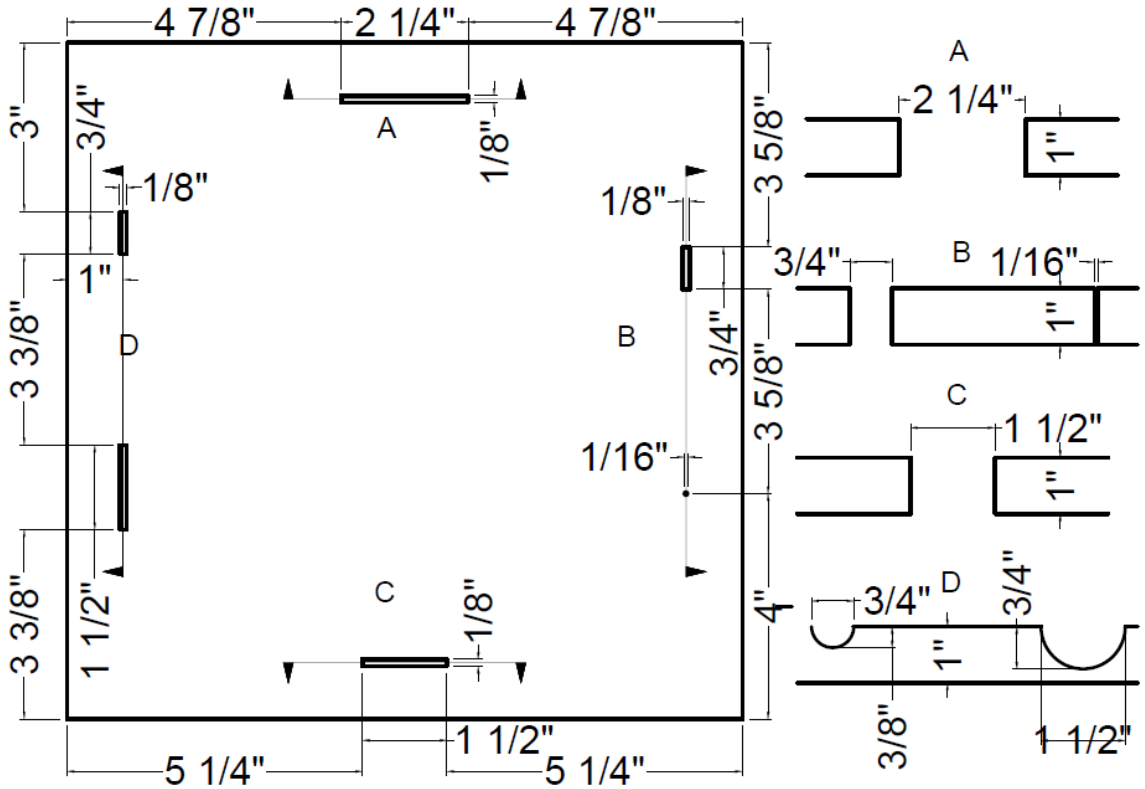
4 7/8"
2 1/4"
4 7/8"
3"
3/4"
1/8"
1"
3 3/8"
D
3 3/8"
1 1/2"
3 3/8"
A
1/8"
1/8"
B
3/4"
1/16"
C
1/8"
3 5/8"
3 5/8"
4"
1 1/2"
5 1/4"
5 1/4"
A
2 1/4"
1"
B
1/16"
3/4"
1"
C
1 1/2"
1"
D
3/4"
3/4"
1"
3/8"
1 1/2"

Figure 3.3 Length-Amplitude specimen design drawings

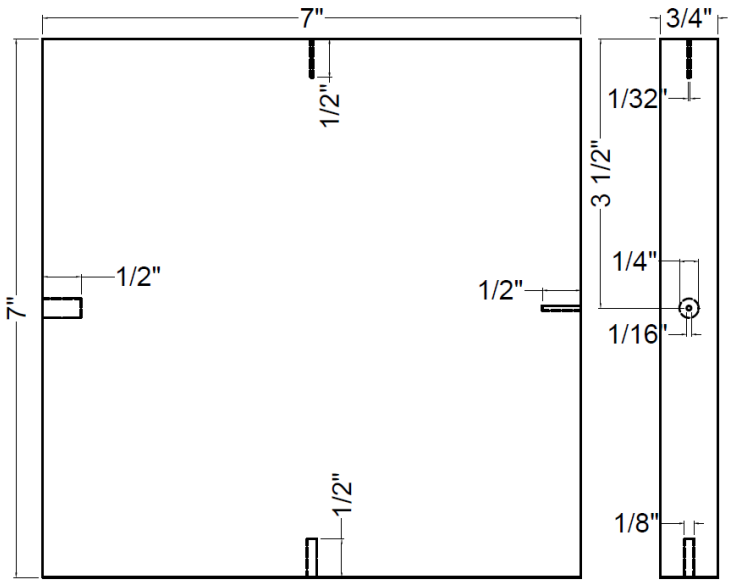

Figure 3.4 Side-drilled hole specimen

The defect size-amplitude test incorporates a ¾" thick, 8"x8", plate of A36 steel with four side drilled holes of ¼", 1/8", 1/16", 1/32" diameters as seen in figure 3.4. Due to the limitations of the machinery, each side-drilled hole was drilled ½" into the plate. The 1/32" hole was chosen because it is near the wavelength at which UT can detect defects (half the wavelength of a 2.25 MHz transducer). The other defects have diameters comparable to the 1/32" hole. The holes are evaluated using an AWS 70° angle beam transducer oriented perpendicular to the defect for maximum reflected amplitude.

3.4.1.3 Transducer Wedge Angle-Amplitude Measurement

The purpose of the transducer angle test is to relate the impact of the angle of the wedge UT transducer to the reflected amplitude.

The AWS UT code requires that up to three different transducer angles are used in the evaluation of steel welds. The code separates every weld into three different zones: the top

quarter, the middle half, and the bottom quarter. 70° angle transducers are used for thin plates, because the beam path, as well as beam spread, can cover the entire volume of the weld. However, thicker welds require deeper angles into the weld to evaluate the top and bottom portion of the weld. The AWS UT procedure adjusts acceptance criteria based on the angle of the transducer. The transducer angle test looks to characterize the impact of transducer angle to the reflected amplitude and evaluate the accuracy of the AWS acceptance criteria.

The SDH1 will be examined using the three AWS angle beam transducers. The 70°, 60°, and 45° angle beam transducers will be oriented perpendicularly to the side drilled holes for maximum amplitudes. These amplitudes should follow the same pattern that is assumed in the AWS UT acceptance criteria.

3.4.1.4 Transducer Orientation-Amplitude Measurement

The purpose of the transducer orientation test is to determine the change in reflected amplitude based on transducer orientation relative to a known defect.

The acceptance criteria in the AWS code require that the maximum reflected amplitude be determined. The AWS allows the ultrasonic transducer to be turned 10° in order to identify defects. As the transducer is turned, the ultrasonic wave reflects off the defect, but the wave reflects a reduced amplitude based on the acoustic wave's beam spread and the angle between defect and transducer. This research looks to quantify the effect of transducer orientation by turning an AWS 70° wedge transducer to various horizontal angles while evaluating known defects.

The four side drilled holes in the SDH is examined using the AWS 70° angle beam transducer. The transducer evaluates each side-drilled hole as it rotates at the same location.

Because of the different sizes of the side-drilled holes, it will also be possible to evaluate the effectiveness of the transducer at identifying small targets at large angles.

3.4.1.5 Defect Orientation-Amplitude Measurement

The purpose of the defect orientation test is to determine the change in reflected amplitude based on defect orientation relative to the transducer wave path.

Defects within steel welds, especially cracks, may consist of several angles. The maximum reflected amplitude occurs when the discontinuity is oriented perpendicular to the transducer, which is parallel to the steel weld, but fatigue cracks are not always oriented parallel to the steel welds. This research looks to quantify the effect of defect orientation by rotating an AWS 70° wedge transducer about the face of known defects.

The four side-drilled holes in the SDH will be examined using the AWS 70° angle beam transducer. The transducer will be rotated around each side-drilled hole while the transducer scans the face of each hole. Because of the different sizes of the side-drilled holes, it will also be possible to evaluate how effective the transducer is at identifying small targets at large angles.

3.4.1.6 Surface Roughness-Amplitude Measurement

The purpose of the surface roughness test is to relate the impact of the surface roughness of a discontinuity to the reflected amplitude.

Unlike radiography, which provides a picture that exposes defects in material, the results from UT does not provide vivid photographic results. UT utilizes shear pulse waves traveling through a material. The reflecting waves from a discontinuity such as the wall of the material or a defect are detected on the oscilloscope as an indication represented by an increase of voltage amplitude. While it is possible to see the approximate orientation of the defect with radiography, UT does not provide the same precision. A drawback of radiography is the reliance of the defect

orientation. If the defect is normal to the radiograph image, no defect would be visible. Defects in steel have sharp edges, and are very jagged with different textures and orientations in varying directions. The surface roughness test specimen is designed to replicate the roughness and various textures comparable to cracks in steel welds. This research looks to determine the effects of discontinuous texture by testing the reflected amplitude of several different types of surface finishes.

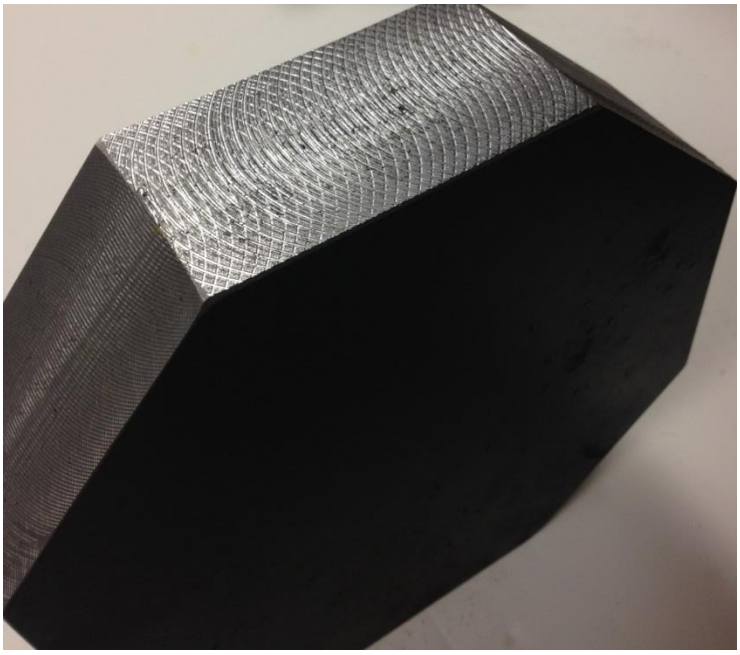

Figure 3.5 Surface roughness specimen

The first test specimen is 2” A36 steel plate with the 2D geometry of an octagon. Each side has a unique surface roughness and finish pattern. The specimen’s surface finish includes: three sides with cross-hatched finishes of different groove distances as seen in figure 3.5, three sides with horizontal finishes of different groove distances, one side with two large grooves cut via grinder to form a horizontal and vertical defect, and the final side with the finest finish available.

The second test specimen is a steel specimen loaned to this research by Dr. Rob Connor. Dr. Connor was developing fatigue cracks in steel plates. The fatigue surfaces are going to be examined and compared to the results of the other surface finishes.

3.4.1.7 Attenuation Measurement

The purpose of the attenuation measurement test is to determine how much reflected amplitude is lost per inch of wave length.

The ultrasonic wave loses energy, which decreases the wave amplitude, as it travels through the steel material. The standard AWS UT code uses an attenuation factor in the identification rating calculation. The AWS attenuation factor is found by subtracting 1 inch from the wave path distance, multiplying the remainder by 2, and rounding to the nearest dB level.

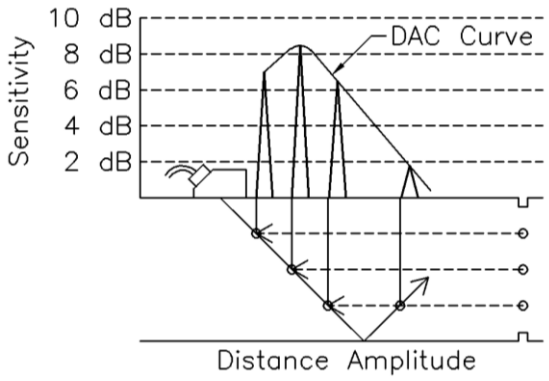

Figure 3.6 AWS Figure S.7 – Shear Wave Distance and Sensitivity Calibration

Additional UT requirements located in the Appendix S of the AWS code use a Distance Amplitude Curve (DAC) to account for the wave attenuation in the steel, as seen in figure 3.6. The DAC calibration is established by measuring three or more 1/16” diameter holes at different wave path lengths within the steel. Indication amplitudes are compared to the DAC rather than using the amplitude factor.

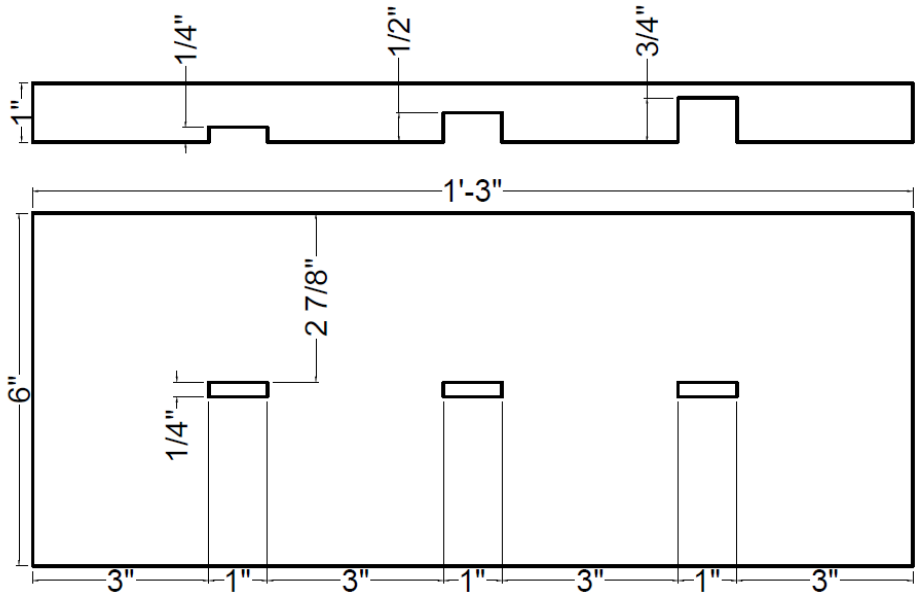

Figure 3.7 Plate with EDM flat, rectangular hole

The test uses two plates with EDM cut holes of varying depths, as seen in figure 3.7. These plates are used to identify the reflected amplitude from the hole surfaces located within the plates. The amplitudes are to be compared to the current AWS Attenuation Factor.

3.4.1.8 Defect Sizing using AWS Procedure-Amplitude Measurement

The purpose of sizing defects in steel welds using the AWS procedure is to evaluate the procedure's effectiveness based on the results and provide suggestions to improve its accuracy.

The standard AWS procedure described in dection 3.2 of this report and the AWS Annex S procedure will be used to evaluate steel specimens with implanted flaws. Four fabricated test plates with implanted flaws of known locations and lengths are used as test specimens for defect sizing. Three plates have transition welds and one plate is a standard butt weld, as seen in figure 3.8.

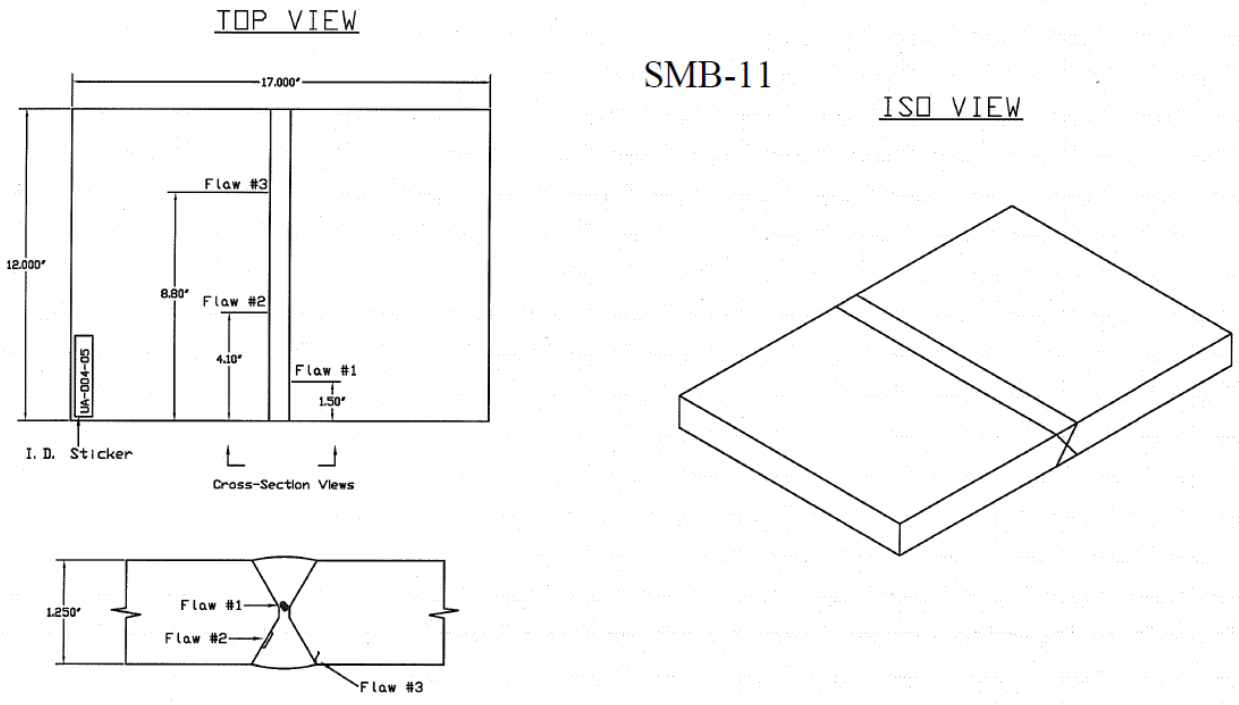

Figure 3.8 Details depicting the SMB 11 plate defect locations

Similar to the length-amplitude test, an encoder will be used to track the waveforms as the transducer moves along the weld. As the defect is scanned, the waveforms are saved to a spreadsheet and associated with the location of the encoder at the time of the scan. The waveforms are then mapped back to the transducer location along the defect length. The visual representation of the waveform along with the defect length is used in the evaluation of the flaw measurement procedures.

3.4.2 Future Work

The tests described herein will be performed using both the UT technology and the phased array UT technology. The results from these tests will be analyzed for the purpose of improving the current AWS UT procedure if necessary, as well as developing a procedure for phased array UT.

3.5 Conclusion

This chapter contains the test procedures that were designed in order to assess both traditional ultrasonic technologies and the phased array technologies. Each test procedure was designed to identify and quantify the unique limitations of the ultrasonic technologies. The test specimens required for all test procedures were designed and manufactured. The initial test setup utilizing the oscilloscope hardware was found to be unsatisfactory, so the USB-UT350 pulser-receiver was ordered in order to provide the encoder capability required for several tests.

Once every test procedure has been completed using the UT technology, the results will be analyzed and the AWS procedure will be updated if necessary. After the UT technology has been analyzed, the specimens will be evaluated using the phased array technology. The results from the phased array technology will be used to develop a phased array UT procedure.

Chapter 4 Vehicle-Mounted Infrared Thermography for Bridge Condition Assessment

The goal of this research task is improve the safety of bridges and tunnels. The objective of the research task is to develop a flexible, portable platform for infrared thermography that enables the technology to be vehicle-mounted for scanning bridge decks, bridge soffits, and tunnels at normal or close to normal traffic speeds. The flexible platform to be developed under the research will mount temporarily to a maintenance vehicle, such that the technology can be shared among maintenance teams in a State Department of Transportation. The platform will also enable the technology to be used in a downward-looking configuration for scanning bridge decks, and an upward-looking configuration to scan bridge soffits for loose concrete at risk of falling into traffic lanes. This unique new technology will provide a new tool for the condition assessment of highway bridges and tunnels.

The flexible platform has been developed, but has not yet been field tested. The unit is shown in figure 4.1.

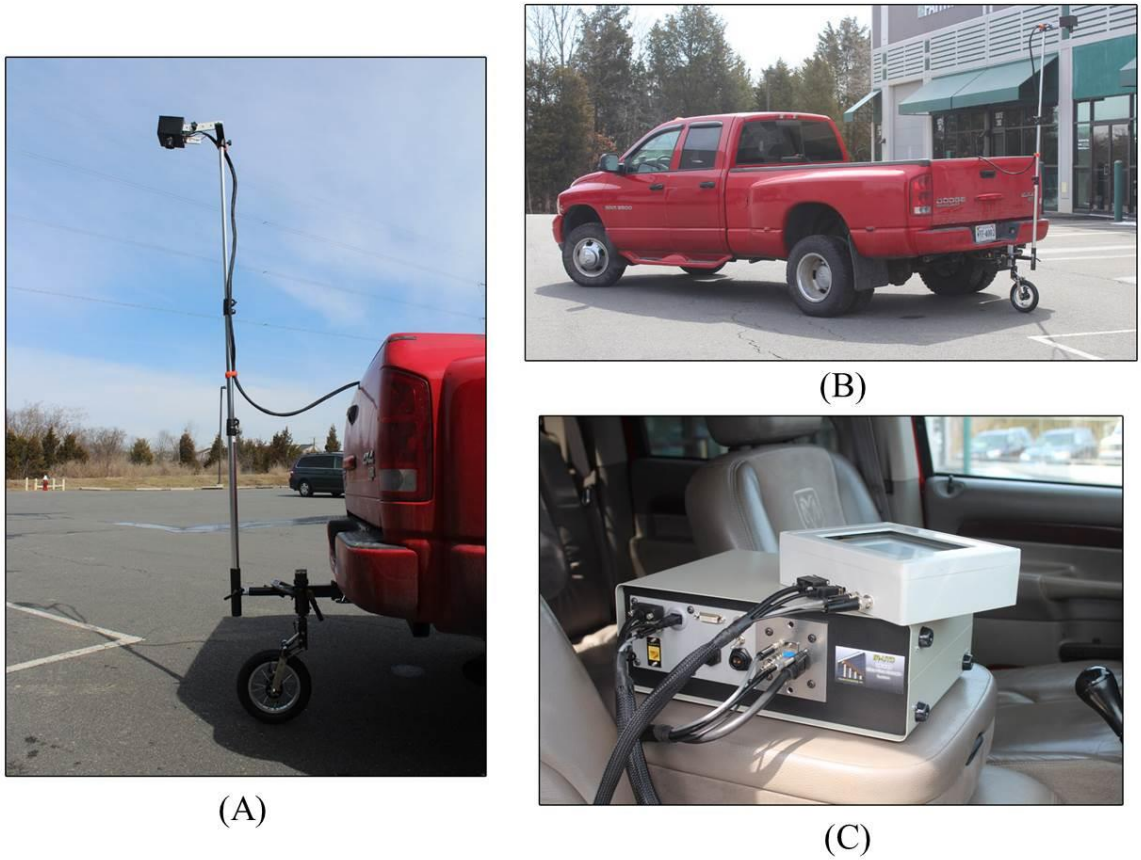

Figure 4.1 Vehicle-mounted infrared unit (a) rear view, (b) side view, (c) close-up view

References

1. Board, N.T.S., *Collapse of I-35W Highway Bridge Minneapolis, Minnesota August 1, 2007*. 2008, National Transportation Safety Board: Washington DC. p. 1, 6, 19, 23, 25, 45, 62, 83,152.

2. Clark, A.V., et al., *Ultrasonic Measurement of Stress in Pin and Hanger Connections.* Journal of Nondestructive Evaluation, 1999. **18**(3): p. 103-113.

3. Klemme, J., *ULTRASONIC STRESS MEASUREMENT FOR EVALUATING THE ADEQUACY OF GUSSET PLATES*, in *Civil and Environmental Engineering*. 2012, University of Missouri-Columbia.

4. Clark, A.V., C.S. Hehman, and T.N. Nguyen, *Ultrasonic Measurement of Stress Using a Rotating EMAT.* Research in Nondestructive Evaluation, 2000. **12**(4): p. 217-240.

5. AWS, *Bridge Welding Code in AWS D1.5*. 2010: Miami, FL.

6. Jessop, T.J., P.J. Mudge, and J.D. Harrison, *Ultrasonic measurement of weld flaw size*, in *NCHRP Report*. 1981.

7. Gruber, G.J., and G.M. Light, *Supplemental Ultrasonic Code Inspection of Structural Weldments*, in *Journal of materials in civil engineering*. 2002. p. p. 57.

8. Shaw Jr, R.E., *Ultrasonic Testing Procedures, Technician Skills and Qualifications.* Jounral of materials in civil engineering, 2002. **14**.

9. Shenefelt, G.A., *Ultrasonic Testing Requirements of the AWS 1069 Building Code and Bridge Specifications.* 1971.

10. Washer, G., Connor, R., and Looten, D., *Performance Testing of Inspectors Implementing NDT Technologies*. 2013, TRB.